ACS APPLIED MATERIALS & INTERFACES

Research Article

www.acsami.org

1-Acetylpyrene–Salicylic Acid: Photoresponsive Fluorescent Organic Nanoparticles for the Regulated Release of a Natural Antimicrobial Compound, Salicylic Acid

Shrabani Barman,[†] Sourav K. Mukhopadhyay,[‡] Krishna Kalyani Behara,[†] Satyahari Dey,*[,‡] and N. D. Pradeep Singh*[,†]

[†]Department of Chemistry and [‡]Department of Biotechnology, Indian Institute of Technology Kharagpur 721302, West Bengal India

Supporting Information

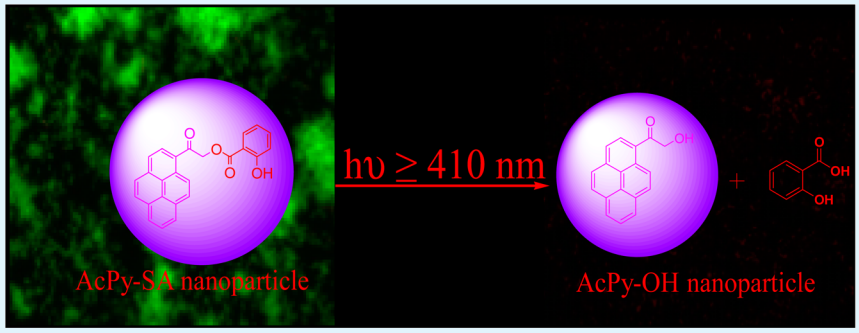

ABSTRACT: Photoresponsive 1-acetylpyrene–salicylic acid (AcPy-SA) nanoparticles (NPs) were developed for the regulated release of a natural antimicrobial compound, salicylic acid. The strong fluorescent properties of AcPy-SA NPs have been extensively used for potential in vitro cell imaging. The phototrigger capability of our newly prepared AcPy-SA NPs was utilized for the efficient release of an antimicrobial compound, salicylic acid. The photoregulated drug release of AcPy-SA NPs has been shown by the subsequent switching off and on of a visible-light source. In vitro biological studies reveal that AcPy-SA NPs of ∼68 nm size deliver the antimicrobial drug salicylic acid into the bacteria cells (*Pseudomonas aeruginosa*) and efficiently kill the cells upon exposure to visible light (≥410 nm). Such photoresponsive fluorescent organic NPs will be highly beneficial for targeted and regulated antimicrobial drug release because of their biocompatible nature, efficient cellular uptake, and light-induced drug release ability.

KEYWORDS: *1-acetylpyrene–salicylic acid, organic nanoparticles, phototrigger, antibiotics, cell imaging, cytotoxicity*

1. INTRODUCTION

Bacterial biofilm formation on implanted medical devices poses a critical clinical problem. Bacterial infections by adherent bacteria have been observed on various medical devices like vascular catheters,[1,2] prosthetic heart valves,[3] urinary catheters,[4−6] cerebrospinal fluid shunts,[7] contact lenses,[8−11] and prosthetic hips,[12] knees,[13] and other orthopedic implants. In general, the most common pathogens involved in biofilm formation are *Staphylococcus aureus*, *Staphylococcus epidermidis*, and *Pseudomonas aeruginosa*. Whitchurch et al.[14] showed that extracellular DNA is a major ingredient of bacterial biofilms formed by the human pathogen *P. aeruginosa*. Once a biofilm is established on the medical device, patients are treated with high doses of antibiotics; however, this method is often found to be unsuccessful, with the only remedy being removal of the implant.

To overcome surgery-related problems, two major strategies have been employed. One is to synthesize new antibiotics, and the other one is to develop novel antibiotic delivery systems that will release in a regulated manner small-molecular-weight antibiotics to prevent bacterial colonization. Recently, nanoparticle (NP)-based delivery systems for the regulated release of antimicrobial drugs in overcoming antibiotics-resistant pathogens have become a promising strategy. Specific types of newly developed NPs for the regulated delivery of antimicrobial drugs include functionalized mesoporous silica,[15] gold nanorods,[16] dendrimers,[17] multicolored fluorescence resonance energy transfer (FRET) silica NPs,[18] and a ZnO/Ag nanohybrid.[19]

In recent times, photoresponsive NPs have attracted great interest for their potential applications, especially in drug[20−29] and gene delivery,[30,31] because of their spatial and temporal control over the release. Photoresponsive nano drug delivery systems (DDSs) are made up of two components: (i) a biocompatible nanocarrier and (ii) a phototrigger. Phototriggers are organic chromophores that perform two major

Received: September 19, 2013
Accepted: May 6, 2014
Published: May 6, 2014

Scheme 1. Photoregulated Delivery of Salicylic Acid by AcPy-SA NPs

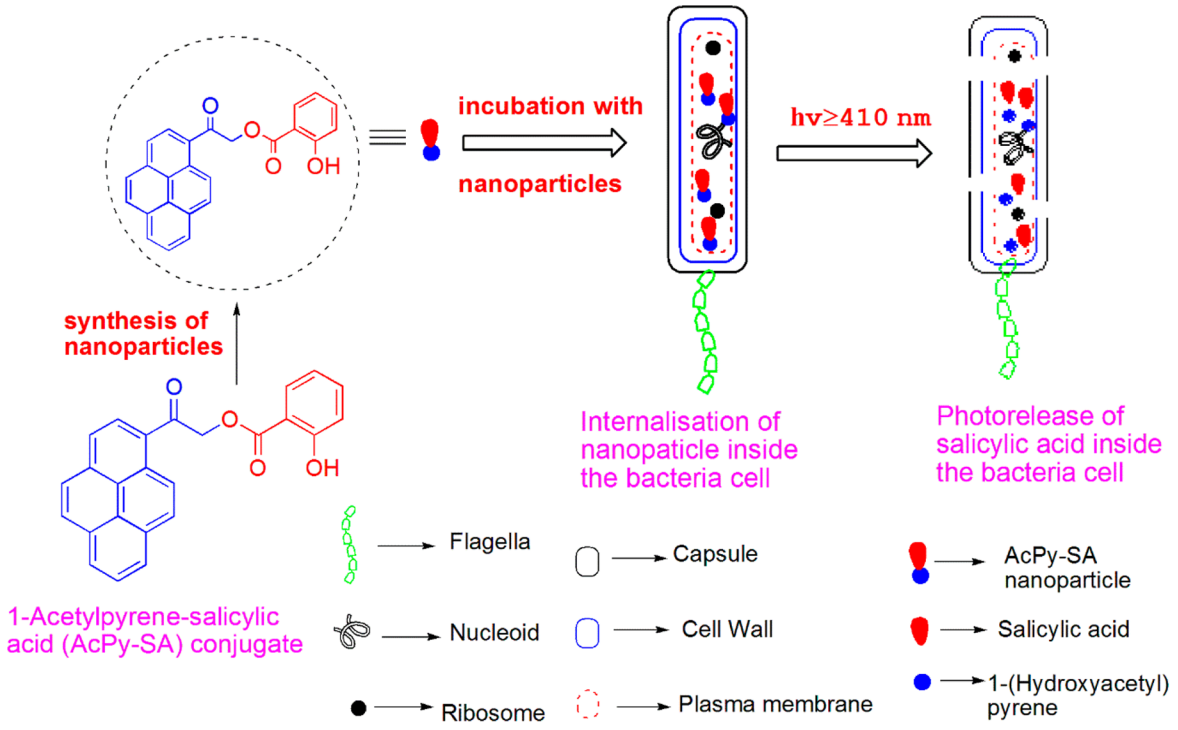

roles: (i) controlled release of a drug and (ii) connection of the drug with the nanocarrier. On the basis of the above approach, Mizukami et al.[32] developed a photocontrolled nano DDS for antibiotics using liposomes as nanocarriers and a coumarin moiety as a phototrigger. The above-developed photoresponsive NPs for antibacterial delivery is a bicomponent system. The major concern with the bicomponent system is loading inefficiency of the drug on the nanocarrier. If the phototriggers themselves can be converted into NPs, then the problem of loading inefficiency can be avoided.

So, herein we aim to design organic NPs that will behave both a nanocarrier and a phototrigger. Recently, our group has reported photoresponsive perylene-3-ylmethanol[33] as a single-component nanocarrier for efficient anticancer drug release in an aqueous medium under visible light. In continuation, we report for the first time the fluorescent NPs of 1-acetylpyrene–salicylic acid (AcPy-SA) as a photoresponsive nanocarrier for regulated in vitro release of a natural antimicrobial, salicylic acid (Scheme 1). For the current study, we have selected plant compound salicylic acid because of its antimicrobial activity against microbial pathogens such as *P. aeruginosa* and *Heliobacter pylori*.[34] Further, salicylic acid is also shown to prevent the attachment of *S. epidermidis* biofilms to polymeric cathedras and attenuating the virulence of *S. aureus*.[35,36]

2. EXPERIMENTAL SECTION

Synthesis of AcPy-SA Conjugate. Salicylic acid (1 equiv) and potassium carbonate (1.2 equiv) were stirred in dry *N*,*N*-dimethylformamide (DMF; 2 mL) for 10 min at room temperature. To the reaction mixture was slowly added 1-(bromoacetyl)pyrene (**2**; 1 equiv), and the mixture was further stirred for 4.5 h. After completion of the reaction, the solvent was removed under reduced pressure, and purification of the crude residue was carried out by column chromatography (petroleum ether:ethyl acetate = 80:20) to give a AcPy-SA conjugate (90%) as a yellow-to-orange solid. Mp: 150–152 °C. ^{1}H NMR ($CDCl_3$, 400 MHz): δ 10.53 (s, 1H), 9.05–9.03 (d, J = 9.6 Hz, 1H), 8.35–8.33 (d, J = 8.4 Hz, 1H), 8.26–8.17 (m, 5H), 8.08–8.05 (t, J = 6.8 Hz, 3H), 7.52–7.48 (d, J = 8 Hz, 1H), 7.03–7.01 (d, J = 8 Hz, 1H), 6.96–6.92 (t, J = 8 Hz, 1H), 5.74 (s, 1H). ^{13}C NMR ($CDCl_3$, 100 MHz): δ 195.2 (1C), 169.7 (1C), 161.9 (1C), 136.3 (1C), 134.8 (1C), 131.1 (1C), 130.6 (1C), 130.5 (1C), 130.3 9 (1C), 128.0 (1C), 127.1 (1C), 126.8 (2C), 126.6 (1C), 126.0 (1C), 125.2 (1C), 124.6 (1C), 124.3 (1C), 124.2 (1C), 124.1 (1C), 119.6 (1C), 117.8 (1C), 112.1 (1C), 68.3 (1C). FTIR (KBr, cm^{-1}): 1720 (OCO), 1638 (CO). UV/vis [EtOH; λ (log ε)]: 356 (4.35), 400 (3.86). HRMS (ES$^+$). Calcd for $C_{25}H_{18}O_4$: m/z 382.1217 ([M + H]$^+$). Found: m/z 382.1219.

Preparation of AcPy-SA and 1-(Hydroxyacetyl)pyrene (AcPy-OH) NPs. Photoresponsive AcPy-SA NPs were prepared by a reprecipitation technique. To 25 mL of water was added slowly for 30 min with constant sonication 5 μL of an acetone solution of a AcPy-SA conjugate (3 mM, 0.0011 g in 1 mL). When the above-mentioned technique was employed, AcPy-OH NPs were also synthesized. The size determination of AcPy-SA and AcPy-OH NPs was carried out using transmission electron microscopy (TEM) and dynamic light scattering (DLS).

Stability of AcPy-SA NPs at Different pHs including Biological pH under Dark Conditions. The stability of AcPy-SA NPs was determined at different pHs including biological pH under dark conditions. Initially, a stock suspension of AcPy-SA NPs was prepared by a reprecipitation technique using 0.0038 g of a AcPy-SA conjugate in 100 mL of water. For pH stability, 20 μL of a suspension of AcPy-SA NPs from a stock solution was dispersed in 1 mL of a phosphate-buffered saline (PBS) solution of different pHs (5.6, 7.4, and 8.0). Similarly, to monitor the AcPy-SA NP stability under the biological environment, the same volume of AcPy-SA NPs from the stock suspension was dispersed in PBS containing a 10% bovine culture medium. All of the samples were stored at 25 ± 2 °C under dark conditions in an airtight container for 6 days. To all of the samples was added 2 mL of acetonitrile, and the resulting mixture was ultrasonicated for 20 min. The samples were then centrifuged, and the supernatants were examined by reverse-phase high-performance liquid chromatography (RP-HPLC) to determine the amount of AcPy-SA NPs decomposed under dark conditions.

Photoinduced Release of Salicylic Acid by AcPy-SA NPs. A total of 0.0038 g of AcPy-SA NPs was dispersed in 100 mL of water

Scheme 2. Synthesis of AcPy-SA Conjugate

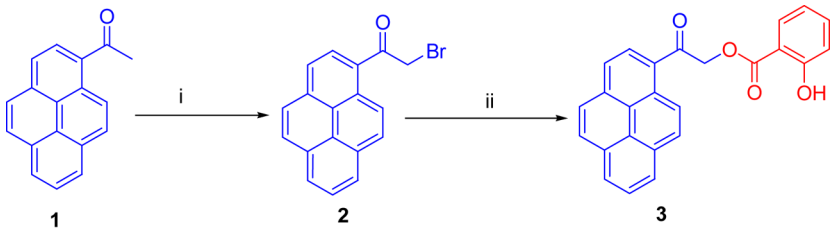

Reagents: i) $CuBr_2$, EtOAC, reflux, 6 h ii) Salicylic acid, K_2CO_3, DMF

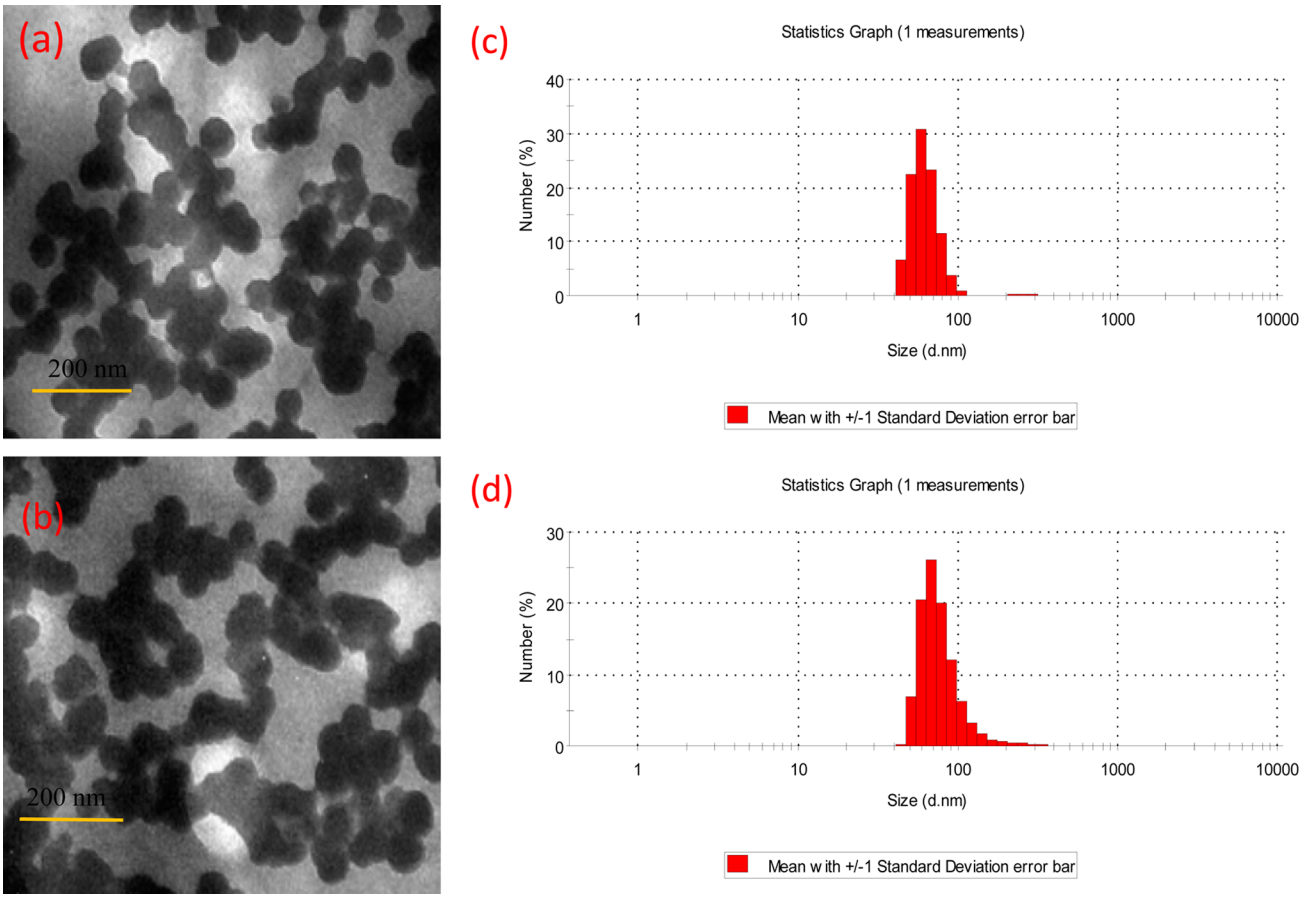

Figure 1. TEM images of (a) AcPy-OH and (b) AcPy-SA and DLS plots of (c) AcPy-OH and (d) AcPy-SA NPs.

and irradiated using a 125 W medium-pressure mercury lamp as the visible-light source (≥410 nm) using a suitable filter (1 M $NaNO_2$ solution; the incident intensity (I_0) is 2.886×10^{16} quanta S^{-1}) with continuous stirring. The progress of photolysis was monitored by taking 0.1 mL aliquots from the photolysate at every 10 min of irradiation, until the reaction reaches 90% conversion. Each 0.1 mL aliquot was then diluted with 0.1 mL of acetonitrile and analyzed by RP-HPLC using acetonitrile as a mobile phase at a flow rate of 1 mL min^{-1}. Detection was performed using a UV-variable wavelength detector at 310 nm. The percentage of decomposed AcPy-SA NPs was determined by calculating the gradual decrease in the peak area of the AcPy-SA NPs. A plot of normalized peak area versus irradiation time obtained from RP-HPLC showed an exponential decrease in the amount of AcPy-SA NPs, indicative of a first-order reaction.

AcPy-OH. Yield: yellow solid. Mp: 86−88 °C. ^{1}H NMR ($CDCl_3$, 200 MHz): δ 9.26 (d, J = 9.4 Hz, 1H), 8.31−8.05 (m, 8H), 5.09 (s, 2H), 3.83 (s, 1H, OH). ^{13}C NMR ($CDCl_3$, 50 MHz): δ 201.3 (1C), 135.2 (1C), 131.1 (1C), 130.8 (1C), 130.6 (2C), 127.2 (1C), 127.1 (2C), 126.8 (2C), 126.7 (1C), 126.3 (1C), 124.7 (1C), 124.3 (2C), 124.1 (1C), 67.0 (1C).

Microorganism and Growth Medium. *P. aeruginosa*-ATCC 27853 was maintained on nutrient agar (NA) plates at 37 °C. The assays were done in a liquid medium.

Antimicrobial Screening: Disk Diffusion Method. The antimicrobial activity was screened by the paper disk diffusion method[37] using NA plates. Sterilized paper disks (6 mm), soaked in a known concentration of the drug, was applied over each of the culture plates previously seeded with 100 μL of an overnight-grown culture of the test organism (*P. aeruginosa*-ATCC 27853). An antibiotic disk of ciprofloxacin was used as the positive control, sterilized paper disks with different phenolic derivatives of benzoic acid (2-hydroxybenzoic acid, 4-hydoxybenzoic acid, and 3,4,5-trihydroxybenzoic acid) along with benzoic acid as tested drugs, and sterilized paper disks without drug or antibiotics were used as negative controls. The experiment was performed in triplicate, and plates were incubated at 37 °C for 18 h. Following incubation, the zones of inhibition formed were measured and the mean diameter was obtained.

Cell Imaging Studies of *P. aeruginosa* Using AcPy-SA NPs. To investigate the cellular internalization of our photoresponsive AcPy-SA NPs, a cell imaging study was carried out. Briefly, *P.*

dx.doi.org/10.1021/am500965n | ACS Appl. Mater. Interfaces 2014, 6, 7045−7054

aeruginosa was grown on 96 well plates (106 well^{-1}) and then incubated with 0.5×10^{-6} M NPs for 18 h at 37 °C. Thereafter, cells were taken by centrifugation at 10000 rpm for 10 min and washed three times with PBS. Imaging was done using a fluorescence microscope (IX 51, Olympus) and a high-performance CCD camera with the appropriate filter using *Image-Pro Discovery 5.1* software.

Antibacterial Activity Assay of AcPy-SA NPs against *P. aeruginosa*. *Before Photolysis.* The antibacterial properties of AcPy-SA NPs were evaluated against *P. aeruginosa*-ATCC 27853 using a broth dilution method.[38] The mid-logarithmic phase bacteria was obtained by growing bacteria in a nutrient broth and then diluted in the same medium to give approximately 10^6 CFU (colony forming units) mL^{-1}. Aliquots (150 μL) of a suspension containing bacteria in a culture medium were added to 150 μL of water containing AcPy-SA NPs, and it was serially diluted from 0.5×10^{-6} to 0.0009×10^{-6} M. The inhibition of growth was determined by measuring the absorbance at 600 nm with a microplate reader after an incubation of 18 h at 37 °C.

After Photolysis. Aliquots (150 μL) of a suspension containing bacteria in a culture medium were added to 150 μL of water containing AcPy-SA NPs, and it was serially diluted from 0.5×10^{-6} to 0.0009×10^{-6} M. Plates were kept at 37 °C for 4 h and then exposed to a medium-pressure mercury lamp (125 W) by placing it 10 cm away from the light source with an appropriate filter (1 M $NaNO_2$ solution; $\lambda \geq 410$ nm; $I_0 = 2.886 \times 10^{16}$ quanta S^{-1}) for 0–20 min. The plate was again incubated at 37 °C for 14 h. The inhibition of growth was determined by measuring the absorbance at 600 nm with a microplate reader.

Live–Dead Assay. Live–dead assay was performed by live/dead Baclight Bacterial Viability Kits (Invitrogen), as per manufacturer protocol. In brief, both the control and visible-light-exposed AcPy-SA NP-treated cells were washed with PBS and 70% ethanol, respectively. Then, this mixture was incubated at 25 °C for 1 h and mixed thoroughly after 15 min of interval. Cells were pelleted by centrifugation at 10000 rpm for 10 min and resuspended in PBS. A total of 3 μL of the dye mixture [SYTO9 and propidium iodide (PI)] was added to each milliliter of a bacterial suspension and incubated at 25 °C in the dark for 15 min. Thereafter, 5 μL of a stained bacterial suspension was trapped between the slide and the 18 mm^2 coverslip. Imaging was done using a fluorescence microscope (IX 51, Olympus) and a high-performance CCD camera with the appropriate filter using *Image-Pro Discovery 5.1* software.

3. RESULTS AND DISCUSSION

Synthesis of AcPy-SA Conjugate. **2** was synthesized by bromination of 1-acetylpyrene (**1**) using $CuBr_2$ in ethyl acetate under reflux for 6 h. Next, treatment of compound **2** with salicylic acid in the presence of potassium carbonate in dry DMF at room temperature yielded a photoresponsive AcPy-SA conjugate (**3**) in good yield, as shown in Scheme 2.

Synthesis and Characterization of AcPy-OH and AcPy-SA NPs. AcPy-OH and AcPy-SA NPs were prepared using a reprecipitation technique, and their sizes were determined by TEM and DLS studies. TEM observation showed that AcPy-OH and AcPy-SA NPs were globular in shape, and their average diameters were found to be ∼44 and ∼55 nm (Figure 1a,b), respectively. DLS studies revealed that the average sizes of AcPy-OH and AcPy-SA NPs were ∼58 and ∼68 nm (Figure 1c,d) respectively, which is slightly bigger than the particle size found by TEM. The surface charge of AcPy-SA NPs was determined by measuring the ζ potential at pH 7.4 (Figure S2 in the Supporting Information, SI). The ζ potential of AcPy-SA NPs is about −48.8 mV. The high negative ζ potential value indicates that AcPy-SA NPs are sufficiently stable in aqueous dispersion and can be used in vitro antimicrobial drug delivery.

Stability of AcPy-SA NPs at Different pHs including Biological pH. The stability of AcPy-SA NPs was assessed in different pH solutions including biological pH. Three different pH solutions (5.6, 7.4, and 8.0) and biological media (10% fetal bovine serum) containing AcPy-SA NPs were stored for a reasonable time period of 6 days at a temperature close to 25 °C under dark conditions. All of the samples were then centrifuged, and the supernatants were examined by RP-HPLC to determine the amount of AcPy-SA NPs decomposed under dark conditions. The result revealed that the AcPy-SA NPs are sufficiently stable under dark conditions in different pH solutions and in different biological media during the study period of 6 days (Table 1).

Table 1. Stability of AcPy-SA NPs at Different pHs and in Different Biological Media

		% of AcPy-SA NPs decomposed under dark conditions after 6 days[a]			
substrate	time (day)	pH 5.6	pH 7.4	pH 8	pH 7.4 (10% FBS)
AcPy-SA NPs	6	7	8	8	6

[a]As examined by RP-HPLC.

UV/Vis Absorption and Fluorescence Properties of AcPy-SA and AcPy-OH NPs. The photophysical properties of AcPy-SA and its phototrigger AcPy-OH NPs were investigated. The UV/vis absorption and emission spectra of a degassed 2×10^{-5} M solution of AcPy-SA and AcPy-OH NPs in water were recorded. Figure 2a & b depict the UV and normalized emission spectra of AcPy-SA NPs, respectively. The AcPy-SA NPs showed λ_{max} around 356 nm with $\varepsilon = 50.0 \times 10^3$ mol^{-1} L cm^{-1}, and their emission maximum was found to be at 405 nm. Similar observations were also noted for AcPy-OH NPs (Figure 2a,b), which indicates that salicylic acid has no significant influence on the UV and fluorescence properties of AcPy-SA NPs. The absorbance of AcPy-SA NPs in the visible-wavelength region along with good fluorescence suggests that AcPy-SA NPs could be suitable for imaging and drug delivery.

Photoinduced Release of Salicylic Acid from AcPy-SA NPs. To investigate the light-induced drug release ability of AcPy-SA NPs, an aqueous suspension of AcPy-SA NPs (10^{-4} M) was photolyzed under visible-light irradiation (≥410 nm). The photorelease of salicylic acid by AcPy-SA NPs was monitored by RP-HPLC. After every 10 min of irradiation, 0.1 mL aliquots were collected from the photolysate, diluted with 0.1 mL of acetonitrile, and analyzed by RP-HPLC. The HPLC overlay chromatogram in Figure 3 shows that, with an increase in the irradiation time, there is a gradual decrease of the peak at $t_R = 4.4$ min, suggesting photocleavage of the AcPy-SA NPs. In addition, we also noted a gradual increase of two new peaks at $t_R = 3.75$ and 2.40 min, corresponding to the photoproducts salicylic acid and AcPy-OH, respectively.

The light-induced release of the antimicrobial drug was then quantified by plotting the HPLC peak area obtained for salicylic acid versus different time intervals of irradiation (Figure 4a). The photolysis was followed until 90% of salicylic acid is released by AcPy-SA NPs. Further, to demonstrate the ability to switch drug delivery on and off through light exposure, we monitored the release of salicylic acid by periodically switching the visible-light source on and off. Figure 4b clearly indicates that whenever the light source was switched off, drug release stopped, which clearly indicates that external stimulus light only induces the antimicrobial drug release.

Antibacterial Activity Studies of AcPy-SA NPs. *Antimicrobial Activity of Salicylic Acid against P. aeruginosa:*

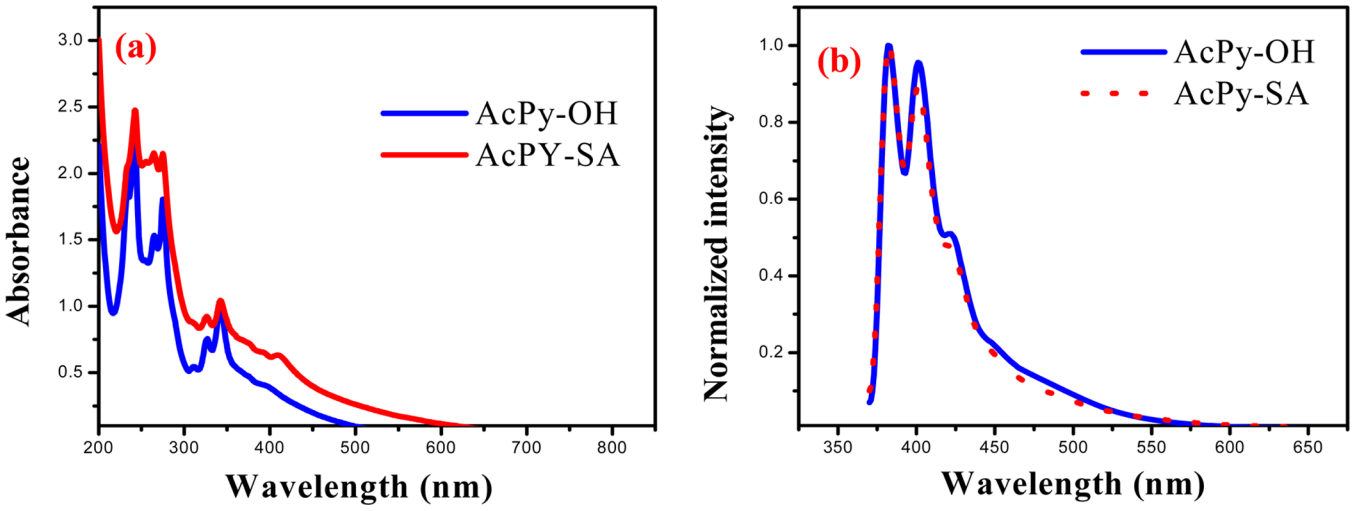

Figure 2. Overlaid spectra of AcPy-OH and AcPy-SA NPs (10^{-5} M): (a) absorption; (b) normalized emission (λ_{ex} = 350 nm).

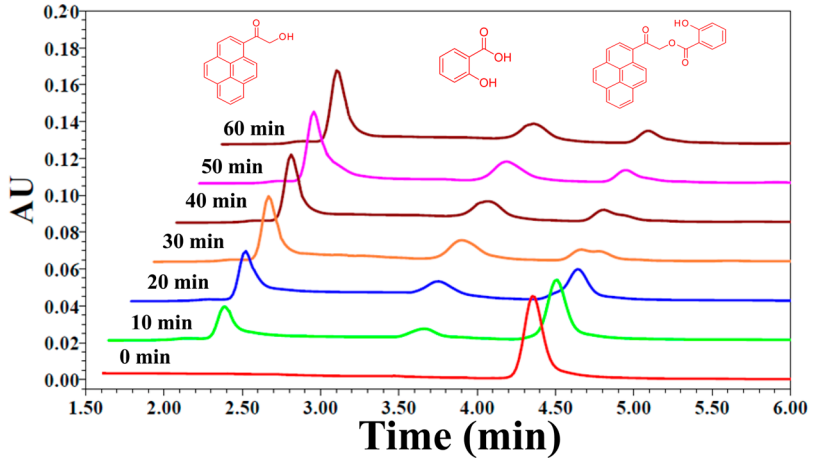

Figure 3. HPLC overlay chromatogram of AcPy-SA NPs at different intervals of light irradiation (≥410 nm).

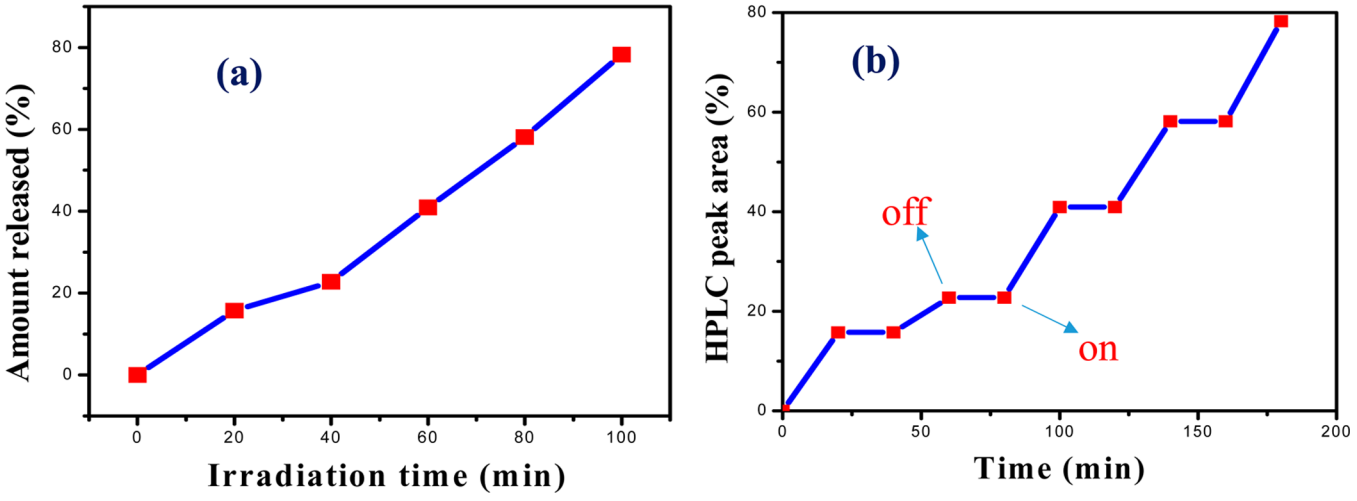

Figure 4. (a) Amount of salicylic acid released from AcPy-SA NPs upon photolysis (≥410 nm) at different time intervals. (b) Release of salicylic acid under bright and dark conditions. "on" and "off" imply the on and off switching of the visible-light source, respectively.

Disk Diffusion Method. In this study, different phenolic derivatives of benzoic acid (2-hydroxybenzoic acid, 4-hydoxybenzoic acid, and 3,4,5-trihydroxybenzoic acid), benzoic acid, and ciprofloxacin (+ control) were tested for antimicrobial susceptibility using the Kirby–Bauer disk diffusion technique on *P. aeruginosa*-ATCC 27853 having a NA plate at 37 °C. Results showed that 2-hydroxybenzoic acid (salicylic acid) exhibited a better inhibitive effect against *P. aeruginosa*-ATCC

dx.doi.org/10.1021/am500965n | ACS Appl. Mater. Interfaces 2014, 6, 7045–7054

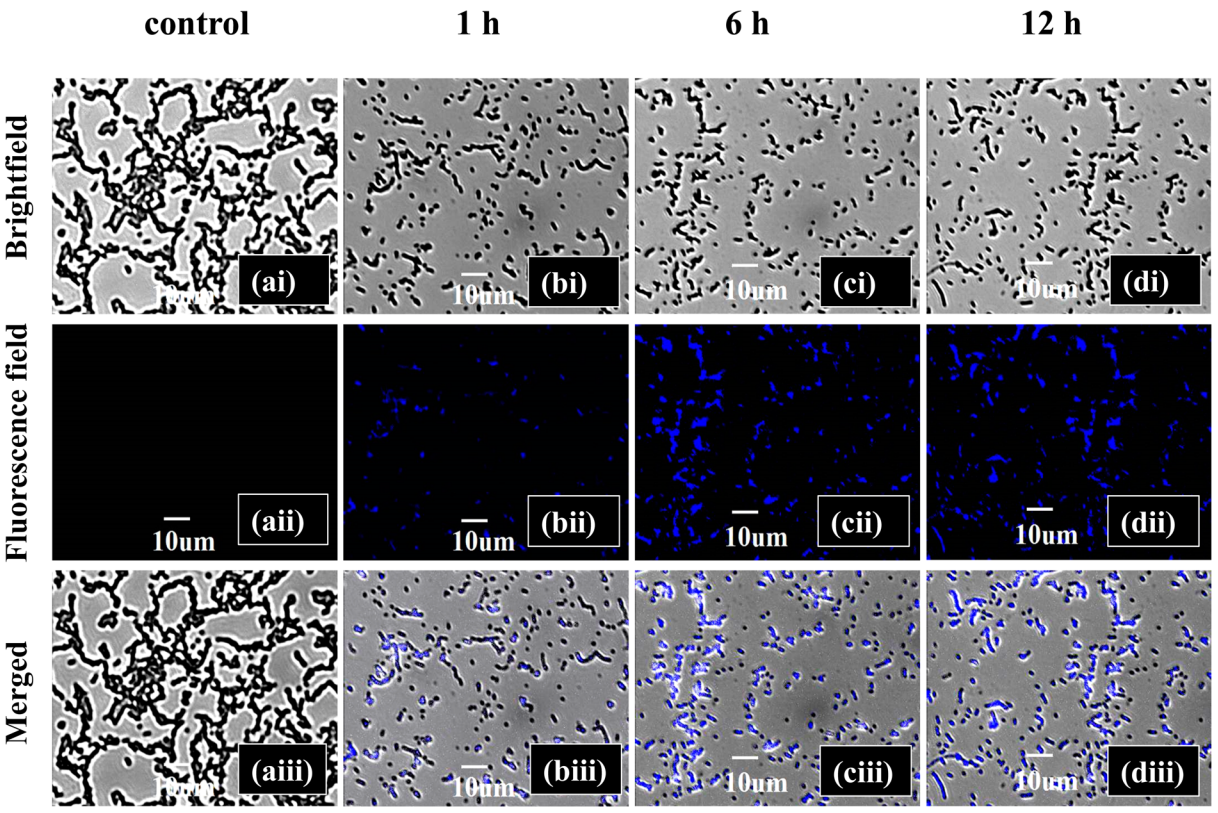

Figure 5. Confocal fluorescence and bright-field images of *P. aeruginosa*-ATCC 27853: (a) untreated cells; (b–d) cells + AcPy-SA NPs (0.5×10^{-6} M) (b) after 1 h, (c) after 6 h, and (d) after 12 h; (i) bright field, (ii) fluorescence (λ_{ex} 430 nm), and (iii) merged.

27853 in comparison to other phenolic derivatives of benzoic acid (Figure S6 in the SI). Hence, for the current study, salicylic acid was undertaken.

Cellular Uptake Studies of AcPy-SA NPs. To understand the cellular internalization behavior of AcPy-SA NPs, we performed cell imaging studies using *P. aeruginosa*-ATCC 27853. After 12 h of incubation, the studies showed that the AcPy-SA NPs were adhered to cell surfaces and internalized by the cell. Further, time-dependent cellular uptake of AcPy-SA NPs was also performed, and the results revealed that, as the incubation time increases, the accumulation of AcPy-SA NPs inside the cell membrane increases. The maximum accumulation of AcPy-SA NPs was noted after 12 h of incubation, as shown by confocal microscopy (Figure 5). However, no fluorescence was observed from the images of the control cells, which implies that there was no autofluorescence of the cells.

Live–Dead Assay of AcPy-SA and AcPy-OH NPs at Regular Intervals of Irradiation. Live–Dead Assay by a Broth Dilution Method. The antibacterial activity of AcPy-SA and AcPy-OH NPs at regular intervals (0–20 min) of visible-light irradiation was evaluated by a broth dilution method. The percentage of cell viability was plotted against the concentration of AcPy-SA NPs at different intervals of irradiation (Figure 6). Exposure of cells incubated with AcPy-SA NPs for a period of 5–20 min using visible light (≥410 nm) resulted in the release of the antimicrobial drug salicylic acid, thereby causing antimicrobial activity against *P. aeruginosa*-ATCC 27853, as validated by CLSI–broth dilution data given in Figure 6. However, minimal cell death was noted when the cells were exposed for 20 min in the presence of phototrigger AcPy-OH NPs or in absence of AcPy-SA NPs, suggesting that the cytotoxicity is mainly due to released salicylic acid.

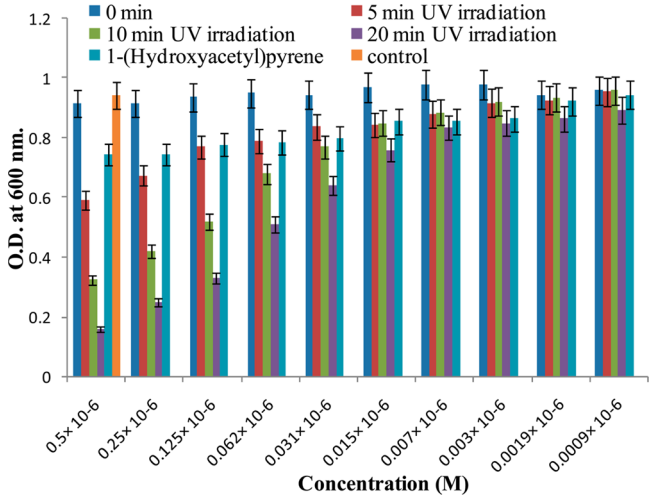

Figure 6. Antibacterial activity of different concentrations of AcPy-SA and AcPy-OH NPs at regular intervals of visible-light irradiation. The culture medium was supplemented with measured at 600 nm after 18 h at 37 ± 2 °C. Data are the mean of triplicate experiments ± S.E.

Live–Dead Assay by Live/Dead Baclight Viability Stain. The viability of bacteria upon exposure to visible light (0-20 min) in the presence of AcPy-SA NPs (0.5×10^{-6} M) was also assessed by fluorescence microscopy (IX 51, Olympus) using the live/dead Baclight viability stain. Live–dead assay was performed by Live/Dead Baclight Bacterial Viability Kits (Invitrogen), as per manufacturer protocol. Two fluorescent dyes were used for bacterial live–dead assay, viz., SYTO9 (480/500) and PI (490/635). Live bacteria having an intact cell membrane fluoresces green upon staining with SYTO9,

dx.doi.org/10.1021/am500965n | ACS Appl. Mater. Interfaces 2014, 6, 7045–7054

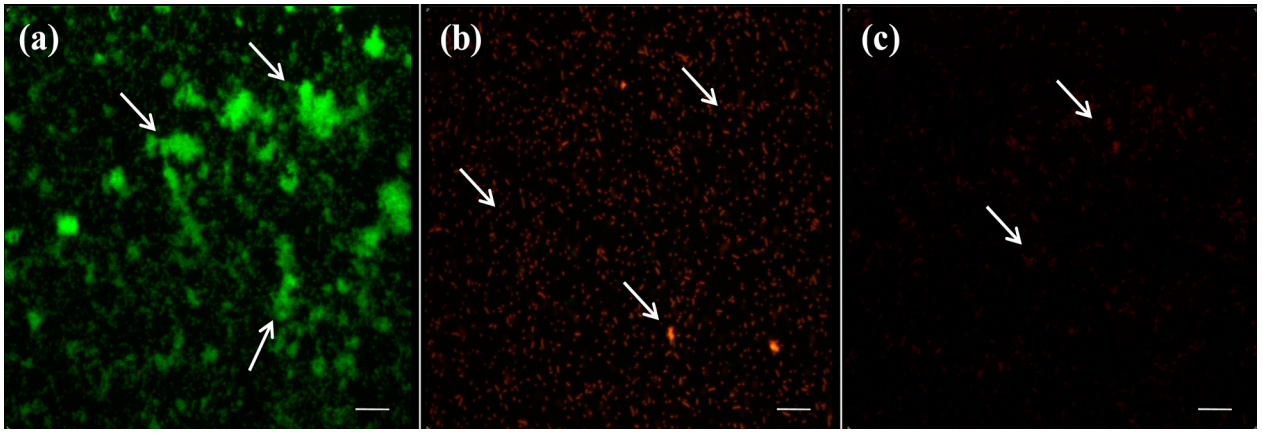

Figure 7. Live/dead Baclight bacterial viability assay on *P. aeruginosa*-ATCC 27853 [a, control; b and c, treated with AcPy-SA NPs (0.5×10^{-6} M) after 10 and 20 min of visible-light irradiation, respectively]. Imaging was done using a fluorescence microscope (IX 51, Olympus) and a high-performance CCD camera using *Image-Pro discovery 5.1* software. The scale bars represent 10 μm.

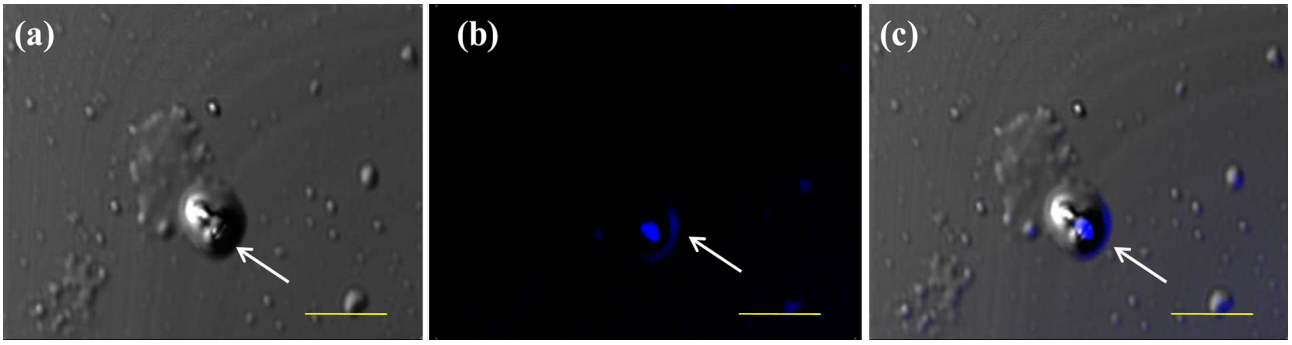

Figure 8. Confocal bright-field and fluorescence images of *P. aeruginosa*-ATCC 27853 incubated with 0.5×10^{-6} M AcPy-SA NPs for 12 h: (a) bright-field image; (b) fluorescence image (λ_{ex} = 430 nm); (c) overlay of parts a and b. The scale bars represent 1 μm.

whereas dead bacteria with a damaged membrane fluoresces red upon staining with PI. The results of this study indicate that the microscopic viability of the cells decreases upon treatment with visible light (10 and 20 min) in the presence of AcPy-SA NPs in comparison to control cells (Figure 7).

Cell death of *P. aeruginosa* by AcPy-SA NPs was also confirmed by cellular imaging studies using confocal microscopy. Figure 8 shows that NPs successively adhere to the bacterial cell membrane and are internalized by the cells.

Microscopic Analysis of AcPy-SA NPs–Bacterial Interaction Using Field-Emission Scanning Electron Microscopy (FESEM) and Atomic Force Microscopy (AFM). NPs designed for DDSs need to be absorbed by the cells at a sufficiently high rate. Literature studies show that the size of the NPs plays a key role in their adhesion and interaction to biological cells. It is presumed that NPs <200 nm are internalized into cells by receptor-mediated endocytosis, while larger particles are taken up by the cell via phagocytosis.[39] In the present study, we can assume that the bacterial cells were found to uptake the AcPy-SA NPs to an adequate extent by receptor-mediated endocytosis because of its smaller size (<100 nm). AcPy-SA NPs adhered to the bacterial membrane has been shown by FESEM (Figure 9) and AFM (Figure 10). Figure 9 shows the FESEM images of bacteria treated with AcPy-SA NPs, in which the NP was found to adhere to the bacterial cell surface (Figure 9f) and resulted in bacterial cell lysis upon visible-light irradiation (Figure 9d,e).

AFM was also used to image the surface topography of bacterial cells at high resolution. The surface of the native cell image was homogeneous and smooth. AcPy-SA NP binding caused a progressive increase in surface roughness. As shown in Figure 10, root-mean-square roughness of bacteria increases from 66.86 to 228.97 nm upon binding of NPs to the bacterial cell surface. AFM analysis also revealed that AcPy-SA NPs bound to the bacterial cell membrane exhibited different surface topographies (Figure 10b) upon visible-light irradiation compared to bacteria alone on the coated glass (Figure 10a).

4. CONCLUSION

We have successfully developed photoresponsive fluorescent organic NPs of AcPy-SA for the regulated release of an antimicrobial drug. AcPy-SA NPs were prepared from a AcPy-SA conjugate by a simple reprecipitation technique. DLS studies revealed that photoresponsive AcPy-SA NPs were ~68 nm in size. Photophysical studies showed that AcPy-SA NPs exhibit good fluorescence and absorbance around 400 nm. We have exploited the fluorescence AcPy-SA NPs for in vitro cell imaging. The regulated release of salicylic acid by AcPy-SA NPs was carried out by exposure to visible light (≥410 nm). Both broth dilution method and live/dead Baclight viability stain studies showed that AcPy-SA NPs kill bacterial cells upon exposure to visible-light irradiation (≥410 nm). Finally, a change in the topography of the bacterial cell membrane by AcPy-SA NPs upon visible-light irradiation was studied using FESEM and AFM. Thus, this work can be a promising starting point in the field of the design and development of single-

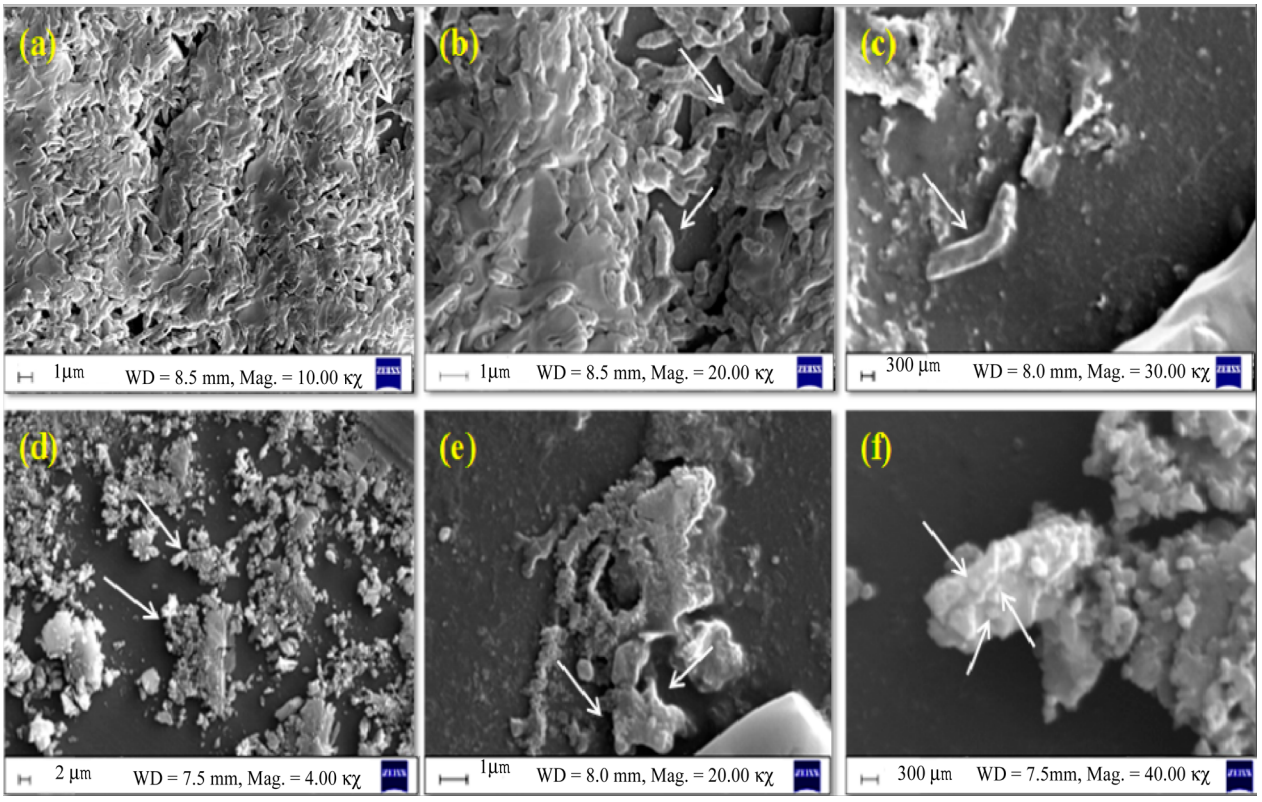

Figure 9. FESEM micrograph of *P. aeruginosa*-ATCC 27853 (a–c, control; d–f, treated with visible light in the presence of AcPy-SA NPs).

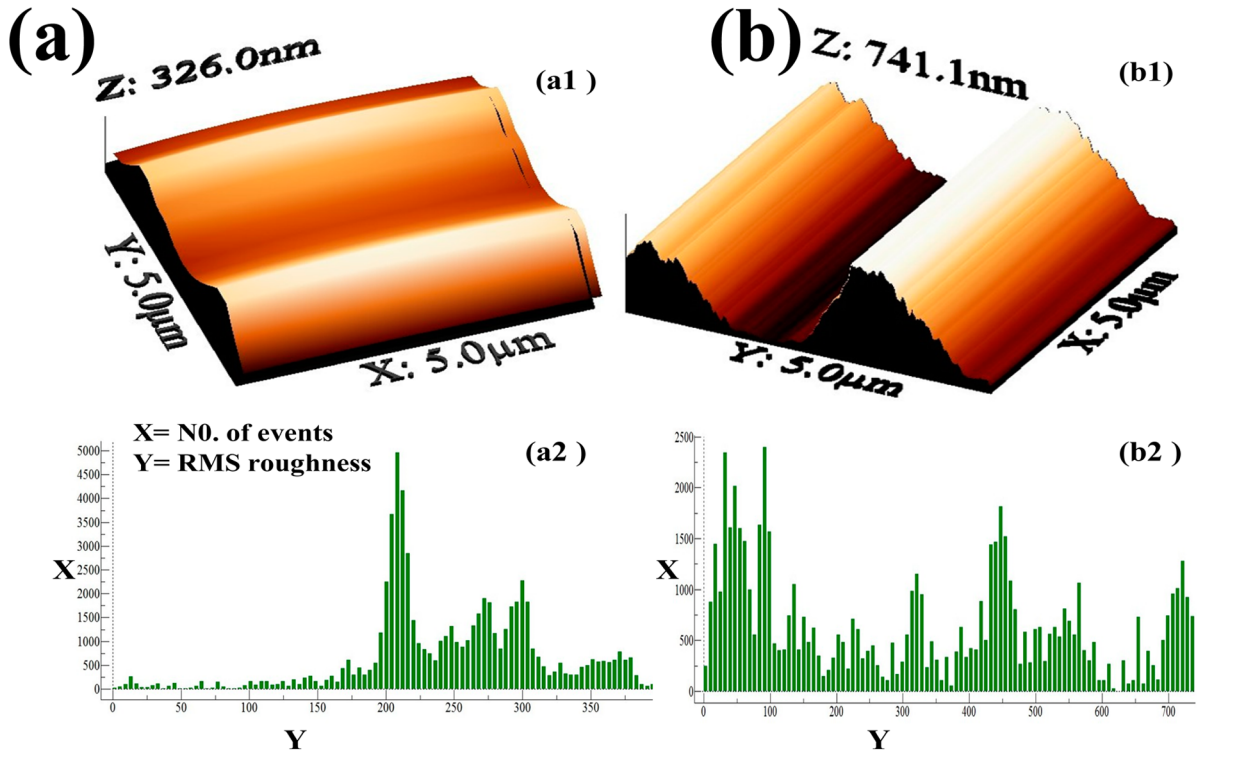

Fig: (a1) control, (b1) treated, (a2) RMS roughness=66.86, (b2) RMS roughness= 228.97

Figure 10. AFM view of *P. aeruginosa*-ATCC 27853. Images were captured using a Multiview-1000 scanning probe microscope at a scan rate of 0.8–1.0 Hz and were first-order flattened. The bacteria appear to be hydrated, and the outer surface appears smooth for bacteria grown (a) without NP and (b) rough-surface-treated with visible light in the presence of AcPy-SA NPs.

dx.doi.org/10.1021/am500965n | *ACS Appl. Mater. Interfaces* 2014, 6, 7045–7054

component photoresponsive organic NPs for targeted and controlled release of antimicrobial drugs.

■ ASSOCIATED CONTENT

Supporting Information

General experimental information, ^{1}H and ^{13}C NMR spectra of AcPy-SA and AcPy-OH, size distribution curves of AcPy-OH and AcPy-SA, ζ potential distribution curve of AcPy-SA NPs, normalized absorption and emission spectra of AcPy-OH and AcPy-SA, CMC determination curve of AcPy-SA, hydrolytic stability of AcPy-SA, antibacterial screening of drugs by a disk diffusion method, and determination of I_0 of the UV lamp. This material is available free of charge via the Internet at http://pubs.acs.org.

■ AUTHOR INFORMATION

Corresponding Authors

*E-mail: sdey@hijli.iitkgp.ernet.in.
*E-mail: ndpradeep@chem.iitkgp.ernet.in.

Notes

The authors declare no competing financial interest.

■ ACKNOWLEDGMENTS

We thank the DST (SERB) for financial support and the DST-FIST for 400 MHz NMR. S.B. is thankful to the Indian Institute of Technology Kharagpur for a fellowship.

■ REFERENCES

(1) Gristina, A. G.; Giridhar, G.; Gabriel, B. L.; Naylor, P. T.; Myrvik, Q. N. Cell Biology and Molecular Mechanisms in Artificial Device Infections. *Int. J. Artif. Organs* **1993**, *16*, 755−764.

(2) Lungren, M. P.; Christensen, D.; Kankotia, R.; Falk, I.; Paxton, B. E.; Kim, C. Y. Bacteriophage K for Reduction of Staphylococcus Aureus Biofilm on Central Venous Catheter Material. *Bacteriophage* **2013**, *3*, e26825.

(3) Litzler, P. Y.; Benard, L.; Barbier-freboury, N.; Villain, S.; Jouenne, T.; Beucher, E.; Bunel, C.; Lemeland, J. F.; Bessou, J. P. Biofilm Formation on Pyrolytic Carbon Heart Valves: Influence of Surface Energy, Roughness, and Bacterial Species. *J. Thorac. Cardiovasc. Surg.* **2007**, *134*, 1025−1032.

(4) Trautner, B. W.; Darouiche, R. O. Role of Biofilm in Catheter-Associated Urinary Tract Infection. *Am. J. Infect. Control* **2004**, *32*, 117−183.

(5) Segev, G.; Bankirer, T.; Steinberg, D.; Duvdevani, M.; Shapur, N. K.; Friedman, M.; Lavy, E. Evaluation of Urinary Catheters Coated with Sustained-Release Varnish of Chlorhexidine in Mitigating Biofilm Formation on Urinary Catheters in Dogs. *J. Vet. Int. Med.* **2013**, *27*, 39−46.

(6) Frank, D. N.; Wilson, S. S.; St. Amand, A. L.; Pace, N. R. Culture-Independent Microbiological Analysis of Foley Urinary Catheter Biofilms. *PLoS One* **2009**, *4*, e7811.

(7) Fux, C. A.; Quigley, M.; Worel, A. M.; Post, C.; Zimmerli, S.; Ehrlich, G.; Veeh, R. H. Biofilm-Related Infections of Cerebrospinal Fluid Shunts. *Clin. Microbiol. Infect.* **2006**, *12*, 331−337.

(8) Imamura, Y.; Chandra, J.; Mukherjee, P. K.; Lattif, A. A.; Szczotka-Flynn, L. B.; Pearlman, E.; Lass, J. H.; O'Donnell, K.; Ghannoum, M. A. Fusarium and Candida Albicans Biofilms on Soft Contact Lenses: Model Development, Influence of Lens Type, and Susceptibility to Lens Care Solutions. *Antimicrob. Agents Chemother.* **2008**, *52*, 171−182.

(9) Wu, Y. T.; Zhu, H.; Willcox, M.; Staplenton, F. Removal of Biofilm from Contact Lens Storage Cases. *Invest. Ophthalmol. Visual Sci.* **2010**, *51*, 6329−6333.

(10) Wiley, L.; Bridge, D. R.; Wiely, L. A.; Odom, J. V.; Elliott, T.; Olson, J. C. Bacterial Biofilm Diversity in Contact Lens-Related Disease: Emerging Role of Achromobacter, Stenotrophomonas and Delftia. *Invest. Ophthalmol. Visual Sci.* **2012**, *53*, 3896−3905.

(11) Abidi, S. H.; Sherwani, S. K.; Siddiqui, T. R.; Bashir, A.; Kazmi, S. U. Drug Resistance Profile and Biofilm Forming Potential of Pseudomonas Aeruginosa Isolated from Contact Lenses in Karachi-Pakistan. *BMC Ophthalmol.* **2013**, *13*, 57−57.

(12) Passerini, L.; Lam, K.; Costerton, J. W.; King, E. G. Biofilm on Indwelling Vascular Catheters. *Crit. Care Med.* **1992**, *20*, 665−673.

(13) Strachan, C. J. The Prevention of Orthopedic Implant and Vascular Graft Infection. *J. Hosp. Infect.* **1995**, *30*, 54−63.

(14) Whitchurch, C. B.; Tolker-Nielsen, T.; Ragas, P. C.; Mattick, J. S. Extracellular DNA Required for Bacterial Biofilm Formation. *Science* **2002**, *295*, 1487−1487.

(15) Knezevic, N. Z.; Trewyn, B. G.; Lin, V. S. Y. Functionalized Mesoporous Silica Nanoparticle-Based Visible Light Responsive Controlled Release Delivery System. *Chem. Commun.* **2011**, *47*, 2817−2819.

(16) Norman, R.S.; Stone, J. W.; Gole, A.; Murphy, C. J.; Sabo-Attwood, T. L. Targeted Photothermal Lysis of the Pathogenic Bacteria Pseudomonas Aeruginosa, with Gold Nanorods. *Nano Lett.* **2008**, *8*, 302−306.

(17) Parelshtein, I.; Ruderman, E.; Perkas, N.; Tzanov, T.; Beddow, J.; Joyce, E.; Mason, T. J.; Blanes, M.; Molla, K.; Patlolla, A.; Frenkel, A. I.; Gedanken, A. Chitosan and Chitosan-ZnO-Based Complex Nanoparticles: Formation, Characterization, and Antibacterial Activity. *J. Mater. Chem. B* **2013**, *1*, 1968−1976.

(18) Wang, L.; Zhao, W.; O'Donoghue, M. B.; Tan, W. Fluorescent Nanoparticles for Multiplexed Bacteria Monitoring. *Bioconjugate Chem.* **2007**, *18*, 297−301.

(19) Ghosh, S.; Goudar, V. S.; Padmalekha, K. G.; Bhat, S. V.; Indi, S. S.; Vasan, H. N. ZnO/Ag Nanohybrid : Synthesis, Characterization, Synergistic Antibacterial Activity and its Mechanism. *RSC Adv.* **2012**, *2*, 930−940.

(20) Agasti, S. S.; Chompoosor, A.; You, C.; Ghosh, P.; Kim, C. K.; Rotello, V. M. Photoregulated Release of Caged Anticancer Drugs from Gold Nanoparticles. *J. Am. Chem. Soc.* **2009**, *131*, 5728−5729.

(21) Angelos, S.; Yang, Y. Y.; Khashab, N. M.; Stoddart, J. F.; Zink, J. I. Dual-Controlled Nanoparticles Exhibiting and Logic. *J. Am. Chem. Soc.* **2009**, *131*, 11344−11346.

(22) Zhu, Y.; Fujiwara, M. Installing Dynamic Molecular Photomechanics in Mesopores: A Multifunctional Controlled-Release Nanosystem. *Angew. Chem., Int. Ed.* **2007**, *46*, 2241−2244.

(23) Lin, Q.; Huang, Q.; Li, C.; Bao, C.; Liu, Z.; Li, F.; Zhu, L. Anticancer Drug Release from a Mesoporous Silica Based Nanophotocage Regulated by Either a One- or Two-Photon Process. *J. Am. Chem. Soc.* **2010**, *132*, 10645−10647.

(24) Lv, C.; Wang, Z.; Wang, P.; Tang, X. Photodegradable Polyurethane Self-Assembled Nanoparticles for Photocontrolled Release. *Langmuir* **2012**, *28*, 9387−9394.

(25) Viger, M. L.; Grossman, M.; Fomina, N.; Almutairi, A. Low Power Upconverted Near-IR Light for Efficient Polymeric Nanoparticle Degradation and Cargo Release. *Adv. Mater.* **2013**, *25*, 3733−3738.

(26) Yan, B.; Boyer, J. C.; Habalt, D.; Branda, N. R.; Zhao, Y. Near Infrared Light Triggered Release of Biomacromolecules from Hydrogels Loaded with Upconversion Nanoparticles. *J. Am. Chem. Soc.* **2012**, *134*, 16558−16561.

(27) Knezevic, N. Z.; Trewyn, B. G.; Lin, V. S. Y. Light- and pH-Responsive Release of Doxorubicin from a Mesoporous Silica Based Nanocarrier. *Chem.—Eur. J.* **2011**, *17*, 3338−3342.

(28) Karthik, S.; Puvvada, N.; Kumar, B. N. P.; Rajput, S.; Pathak, A.; Mondal, M.; Singh, N. D. P. Photoresponsive Coumarin-Tethered Multifunctional Magnetic Nanoparticles for Release of Anticancer Drug. *ACS Appl. Mater. Interfaces* **2013**, *5*, 5232−5238.

(29) Karthik, S.; Saha, B.; Ghosh, S. K.; Singh, N. D. P. Photoresponsive Quinoline Tethered Fluorescent Carbon Dots for Regulated Drug Delivery. *Chem. Commun.* **2013**, *49*, 10471−10473.

(30) Liu, G.; Dong, C. M. Photoresponsive Poly(*S*-(*o*-nitrobenzyl)-L-cysteine)-*b*-PEO from a L-Cysteine *N*-Carboxyanhydride Monomer:

Synthesis, Self-Assembly, and Phototriggered Drug Release. *Biomacromolecules* **2012**, *13*, 1573−1583.
(31) Liu, Y. C.; Ny, A. L. M. L.; Schmidt, J.; Talmon, Y.; Chmelka, B. F.; Lee, C. T., Jr. Photo-Assisted Gene Delivery Using Light-Responsive Catanionic Vesicles. *Langmuir* **2009**, *25*, 5713−5724.
(32) Mizukami, S.; Hosoda, M.; Satake, T.; Okada, S.; Hori, Y.; Furuta, T.; Kikuchi, K. Photocontrolled Compound Release System Using Caged Antimicrobial Peptide. *J. Am. Chem. Soc.* **2010**, *132*, 9524−9525.
(33) Jana, A.; Devi, K. S. P.; Maiti, T. K.; Singh, N. D. P. Perylene-3-ylmethanol: Fluorescent Organic Nanoparticles as a Single-Component Photoresponsive Nanocarrier with Real-Time Monitoring of Anticancer Drug Release. *J. Am. Chem. Soc.* **2012**, *134*, 7656−7659.
(34) Halim, V. A.; Eschen-Lippold, L.; Altmann, S.; Birschwilks, M.; Scheel, D.; Rosahl, S. Salicylic Acid is Important for Basal Defense of Solanum Tuberosum against Phytophthora Infestans. *Mol. Plant−Microbe Interact.* **2007**, *20*, 1346−1352.
(35) Polonio, R. E.; Mermel, L. A.; Paquette, G. E.; Sperry, J. F. Eradication of Biofilm-Forming Staphylococcus Epidermidis (RP62A) by a Combination of Sodium Salicylate and Vancomycin. *Antimicrob. Agents Chemother.* **2001**, *45*, 3262−3266.
(36) Kupferwasser, L. I.; Yeaman, M. R.; Nast, C. C.; Kupferwasser, D.; Xiong, Y. Q.; Palma, M.; Cheung, A. L.; Bayer, A. S. Salicylic Acid Attenuates Virulence in Endovascular Infections by Targeting Global Regulatory Pathways in Staphylococcus Aureus. *J. Clin. Invest.* **2003**, *112*, 222−233.
(37) Wiegand, I.; Hilpert, K.; Hancock, R. E. W. Agar and Broth Dilution Methods to Determine the Minimal Inhibitory Concentration (MIC) of Antimicrobial Substances. *Nat. Protoc.* **2008**, *3*, 163−175.
(38) Bauer, A. W.; Kirby, W. M. M.; Sherris, J. C.; Turch, M. Antibiotic Susceptibility Testing by a Standardized Single Disk Method. *Am. J. Clin. Pathol.* **1966**, *45*, 493−496.
(39) Brayner, R.; Ferrari-lliou, R.; Brivois, N.; Djediat, S.; Benedetti, M. F.; Fievet, F. Toxicological Impact Studies Based on Escherichia Coli Bacteria in Ultrafine ZnO Nanoparticles Colloidal Medium. *Nano Lett.* **2006**, *6*, 866−870.